Supporting Information

Room-temperature Barbier single-atom polymerization induced emission as a versatile approach for the utilization of monofunctional carboxylic acid resources

Quan-Xi Shi,[a,b] Qian Li,[a,b] Hang Xiao,[b,c] Xiao-Li Sun,[c] Hongli Bao[b] and Wen-Ming Wan*[a,b]

a. College of Chemistry, Fuzhou University, Fuzhou, 350108, P. R. China
b. State Key Laboratory of Structural Chemistry, Key Laboratory of Coal to Ethylene Glycol and Its Related Technology, Center for Excellence in Molecular Synthesis Fujian Institute of Research on the Structure of Matter, Chinese Academy of Sciences, 155 West Yangqiao Road, Fuzhou 350002, P. R. of China
c. College of Environmental Science and Engineering, Engineering Research Center of Polymer Green Recycling of Ministry of Education, Fujian Key Laboratory of Pollution Control &Resource Reuse, Fujian Normal University, Fuzhou, 350007, P. R. China.

Tables of Contents

Experimental details

Materials

THF was dried with sodium metal before use, and re-evaporated and purified with benzophenone as an indicator. Chemicals and other common reagents were obtained from commercial suppliers and used without further purification.

Characterization methods

Nuclear magnetic resonance (NMR) spectroscopy. The ^{1}H and ^{13}C NMR measurements were performed on Bruker-BioSpin AVANCE III HD 400 spectrometer in $CDCl_3$ using tetramethylsilane as an internal standard.

Gel permeation chromatography (GPC). Weight-average molecular weight (M_w) and polydispersity indices (PDI) of the polymers were estimated on an Agilent 1260 Infinity Ⅱ equipped with a G7110B isocratic pump and G7162A refractive index detector. Polystyrene standards were utilized, and DMF was used as the eluent at a flow rate of 1.0 mL/min at 50 ^{o}C.

Fourier transform infrared (FT-IR) spectroscopy. FT-IR Spectra using KBr pellets were recorded on a TENSOR II FTIR Spectrometre (Bruker, Germany). The spectra were recorded from an accumulation of 16 scans in the range of 4000-400 cm^{-1} and were collected at room temperature. The OPUS v7.5 software auto-corrected the spectral base line and calculated the second derivative spectra.

UV-vis absorption. The spectra were recorded in THF with sample concentration of 0.1 mg/mL and sample transmittance at 500 nm were acquired in THF/Water mixtures with different water fractions (f_w, vol%) on a Shimadzu UV-2450 UV-Vis spectrophotometer at room temperature.

Luminescence spectroscopy. The spectrum was performed on a Shimadzu RF 5301pc fluorescence spectrophotometer in a quartz cuvette with a path length of 1 cm.

Aggregation-induced emission (AIE) property. The measurements of the polymer in solvent/nonsolvent mixtures were tested. In this study, THF was selected as good solvent for polymers and water as aggregation-inducing nonsolvent. The luminescence spectra of polymers in THF/Water mixtures with different water content were recorded respectively on a Shimadzu RF-5301pc fluorescence spectrophotometer.

Artificial light-harvesting system property. The artificial light-harvesting system were prepared by casting the mixture of different mass ratio of PTPM (10 mg/mL in THF) / NiR (1.0 mg/mL in THF) onto a quartz sheet followed by evaporation of the solvent. The spectra were recorded on the Shimadzu RF-5301pc fluorescence spectrophotometer.

The detection of 2,4,6-trinitrotoluene (TNT). The detection was performed by luminescence quenching of aggregated polymer in the THF/Water mixtures. The luminescence spectra (excitation @ 386 nm) of polymer solution (0.1 mg/mL in water/THF mixtures with 90% water fractions (vol%)) upon addition of different amounts of TNT were tested. Thus, the intensities and quenching ratio (the luminescence quenching efficiency = $(1- I/I_0) \times 100\%$, I and I_0 denote the luminescence intensity of polymer with and without TNT, respectively) of polymer solution upon addition of different amounts of TNT were acquired. Further, Corresponding Stern–Volmer plots of TNT was acquired, which can be used to detect the content of TNT. Meanwhile, test strips for the detection of TNT were made by dripping PTPM solution onto the filter papers and then dried it in air which showed yellow luminescence under irradiation with UV lamp @ 365 nm. Take the TNT solution and add it dropwise to the prepared test paper. After the solvent evaporates, there is no emission under UV lamp @365nm, and the minimum detection limit visible to the human eye is 100ng. (taking 1 μL of 0.1mg/mL TNT solution in methanol).

Theoretical calculation. All the molecules were fully optimized by density functional theory (DFT) methods with the B3LYP hybrid functional and the 6-311G* basis set implemented in the Gaussian 09 package. The vertical excitations and the excited state structure optimizations were performed using the time-dependent extension of DFT (TD-DFT) with the same functional and basis set. The environment layer is treated with the universal force field (UFF). All the atoms are allowed to relax both in the ground and excited state calculations.

Safety precautions.

Note1: The highly explosive TNT should be used with extreme caution and handled only in small quantities, open fire and impact shall be avoided during use and abandoned TNT should dilute with a large amount of water for post-treatment.

Note2: The BPO is highly oxidizing, flammable and explosive, and shall avoid impact and violent vibration during use。

Synthetic procedures

Synthesis of *p*-PTPM. To one flame-dried Schlenk tube containing freshly peeled Mg scraps (0.3 g, 4.8 equivalent), was added 1.4-dibromobenzene (1.23 g, 2.0 equivalent), benzoyl peroxide (0.63 g ,1.0 equivalent) dissolved in THF (10 mL) at room temperature through a syringe. After reaction for 24 h, the solution was quenching and hydrolysis with 20 mL saturated aqueous ammonium chloride. After filtration and workup with dichloromethane / water, the organic solution was dried with anhydrous $MgSO_4$ and concentrated under reduced pressure. After the product was purified by precipitation into excessive petroleum ether, filtered and dried under vacuum, 0.657 g *p*-PTPM was obtained as a light-yellow powder with a yield of 68.6%. ^1H NMR (400 MHz, $CDCl_3$): δ=7.89-7.22 (broad, -C_6H_5-, 5H), 7.22-6.76 (broad, -C6H4-, 4H), 4.02-3.12 (broad, -OH, 1H).

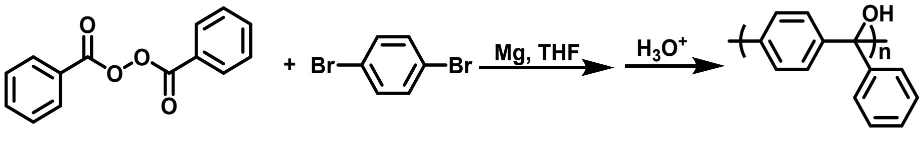

Synthesis of *p*-PPTPM. To one flame-dried Schlenk tube containing freshly peeled Mg scraps (0.3 g, 4.8 equivalent), was added 4,4-dibromobiphenyl (1.63 g, 2.0 equivalent), benzoyl peroxide (0.63 ,1.0 equivalent) dissolved in THF (10 mL) at room temperature through a syringe. After reaction for 24 h, the solution was quenching and hydrolysis with 20 mL saturated aqueous ammonium chloride. After filtration and workup with dichloromethane / water, the organic solution was dried with anhydrous $MgSO_4$ and concentrated under reduced pressure. After the product was purified by precipitation into excessive petroleum ether, filtered and dried under vacuum, 0.862 g *p*-PPTPM was obtained as a light-yellow powder with a yield of 63.7 %. ^1H NMR (400 MHz, $CDCl_3$): δ=8.13-763 (broad, -C_6H_5, 5H), 7.63-6.87 (broad, -C_6H_4-, 8H), 4.12-3.04 (broad, -OH, 1H).

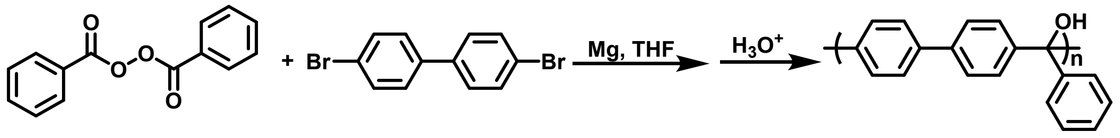

Synthesis of *o*-PTPM. To one flame-dried Schlenk tube containing freshly peeled Mg scraps (0.3 g, 4.8 equivalent), was added 1,2-dibromobenzene (1.23 g, 2.0 equivalent), benzoyl peroxide (0.63 ,1.0 equivalent) dissolved in THF (10 mL) at room temperature through a syringe. After reaction for 24 h, the solution was quenching and hydrolysis with 20 mL saturated aqueous ammonium chloride. After filtration and workup with dichloromethane / water, the organic solution was dried with anhydrous $MgSO_4$ and concentrated under reduced pressure. After the product was purified by precipitation into excessive petroleum ether, filtered and dried under vacuum,0.401 g *o*-PTPM was obtained as a light-yellow powder with a yield of 41.7 %. ^{1}H NMR (400 MHz, $CDCl_3$): δ=8.15-6.59 (broad, -C_6H_5-, -C_6H_4-, 9H), 4.12-3.02 (broad, -OH, 1H).

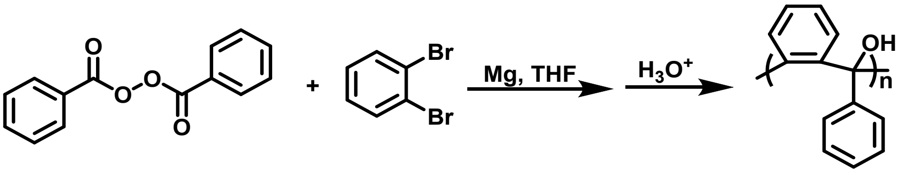

Synthesis of *m*-PTPM. To one flame-dried Schlenk tube containing freshly peeled Mg scraps (0.3 g, 4.8 equivalent), was added 1,3-dibromobenzene (1.23 g, 2.0 equivalent), benzoyl peroxide (0.63 ,1.0 equivalent) dissolved in THF (10 mL) at room temperature through a syringe. After the reaction was refluxed for 24 h, the solution was cooled to room temperature, followed by quenching and hydrolysis with 20mL saturated aqueous ammonium chloride. After filtration and workup with dichloromethane/ water, the organic solution was dried with anhydrous $MgSO_4$ and concentrated under reduced pressure. After the product was purified by precipitation into excessive petroleum ether, filtered and dried under vacuum, 0.512 g *m*-PTPM was obtained as a light-yellow powder with a yield of 53.2 %. ^{1}H NMR (400 MHz, $CDCl_3$): δ=7.98-7.22 (broad, -C_6H_5-,5H), 7.22-6.79 (broad, -C_6H_4-, 4H),4.12-3.19 (broad, -OH, 1H).

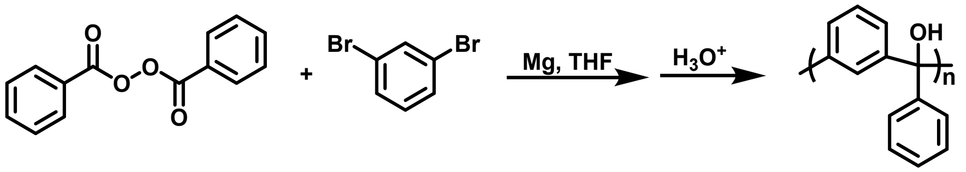

Synthesis of benzoyl peroxide (BPO). To one round bottom flask was added benzoic acid (1g, 1 equivalent), *N*,*N*-dimethyl-4-pyridinamine (DMPA) (0.1g, 0.1 equivalent), then add hydrogen peroxide (H_2O_2) (1.2mL, 1.1 equivalent) in an ice water bath, stir well and slowly add *N*,*N*-diisopropylcarbodiimide (DIC) dropwise (1.4 mL, 1.1 equivalent), continue the reaction for two hours under ice-water bath. The reaction solution was extracted three times with dichloromethane, and the organic phases were combined and dried with anhydrous $MgSO_4$. Then the solvent was removed by rotary evaporation under vacuum and the residue was chromatographed on silica gel (petroleum ether/ethyl acetate = 10:1) to yield BPO. (0.95g, 95.6%).

^{1}H NMR (400 MHz, $CDCl_3$): δ=8.09 -8.07 (d, ArH,2H), 7.68-7.64 (t, ArH, 4H), 7.53-7.49 (t, ArH, 4H). ^{13}C NMR (100 MHz, $CDCl_3$): δ=163.10 (CO), 134.32 (ArCH), 129.82 (ArCH), 128.89 (ArCH), 125.65 (ArC).

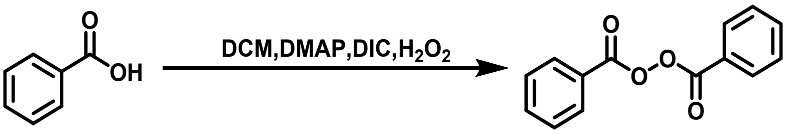

Synthesis of triphenylmethanol (TPM). To one flame-dried Schlenk tube containing freshly peeled Mg scraps (0.24 g, 4.8 equivalent), was added bromobenzene (1.3 g, 4.0 equivalent), benzoyl peroxide (0.5g ,1.0 equivalent) dissolved in THF (10 mL) at room temperature through a syringe. After reaction for 12 h, the reaction solution was extracted three times with dichloromethane, and the organic phases were combined and dried with anhydrous $MgSO_4$. Then the solvent was removed by rotary evaporation under vacuum and the residue was chromatographed on silica gel (petroleum ether/ethyl acetate = 10:1) to yield TPM. (0.85g, 79.4%).^{1}H NMR (400 MHz, $CDCl_3$): δ=7.39-7.21 (m, Ar-H, 15H), 2.80 (s, -OH, 1H). ^{13}C NMR (100 MHz, $CDCl_3$): δ=146.85 (ArC), 127.93 (ArCH), 127.92 (ArCH), 127.26 (ArCH), 82.05 (COH).

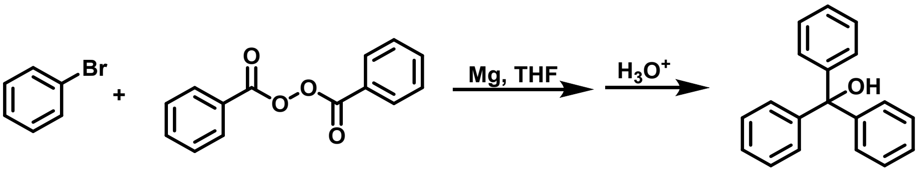

Synthesis of 4,4'-dimethyltriphenylmethanol. To one flame-dried Schlenk tube containing freshly peeled Mg scraps (0.24 g, 4.8 equivalent), was added 4-bromotoluene (1.4 g, 4.0 equivalent), benzoyl peroxide (0.5g ,1.0 equivalent) dissolved in THF (10 mL) at room temperature through a syringe. After reaction for 12 h, the reaction solution was extracted three times with dichloromethane, and the organic phases were combined and dried with anhydrous $MgSO_4$. Then the solvent was removed by rotary evaporation under vacuum and the residue was chromatographed on silica gel (petroleum ether/ethyl acetate = 10:1) to yield 4,4'-dimethyltriphenylmethanol. (0.82g, 71.4%).^{1}H NMR (400 MHz, $CDCl_3$): δ=7.31-7.25 (m, Ar-H, 8H), 7.16-7.11 (m, Ar-H, 5H),2.74 (s, OH,1H),2.34 (s, CH_3,6H). ^{13}C NMR (100 MHz, $CDCl_3$): δ=147.24 (ArC), 144.28 (ArC), 136.96 (ArC), 128.71 (ArCH) , 128.17 (ArCH), 127.96 (ArCH), 127.93 (ArCH), 127.21 (ArCH), 81.86 (COH), 21.15 (CH_3).

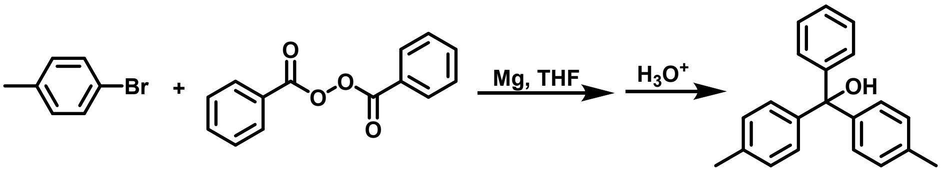

Result characterization data

Synthetic characterization

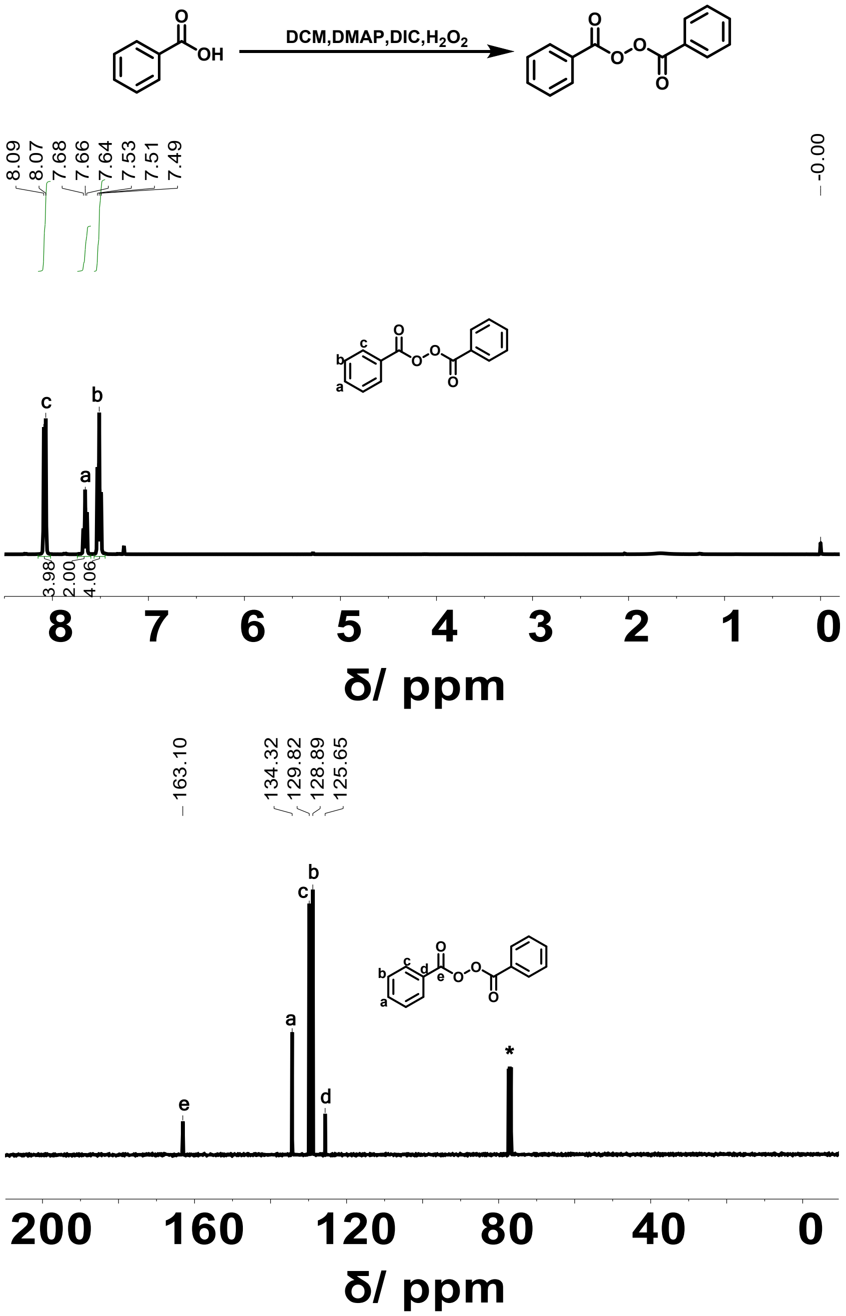

Figure S1. The strategy of converting benzoic acid to benzoyl peroxide and the ^{1}H (400 MHz) NMR and ^{13}C (100 MHz) NMR spectrum of benzoyl peroxide in CDCl$_3$. The solvent peaks are marked with asterisks.

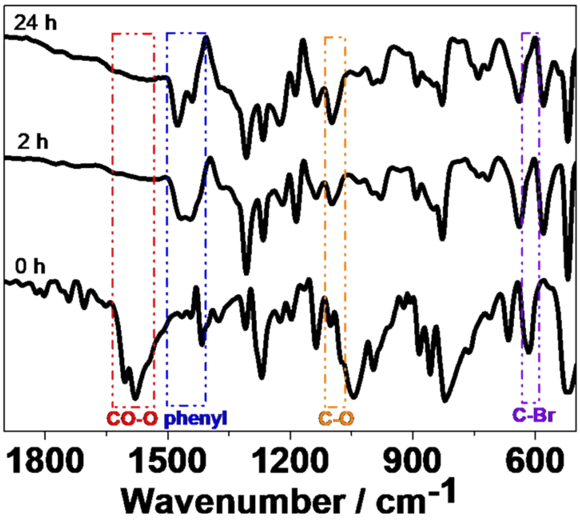

Figure S2. FT-IR spectra of polymerization kinetics.

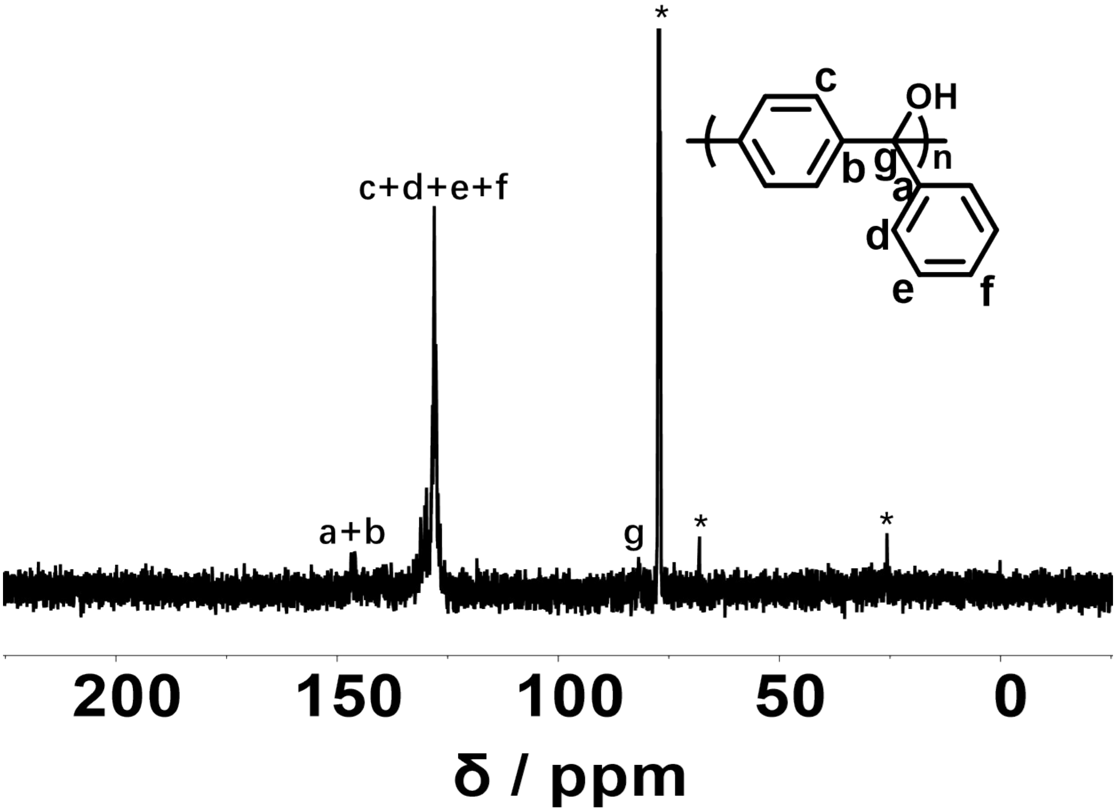

Figure S3. ^{13}C (100 MHz) NMR spectrum of *p*-PTPM in $CDCl_3$. The solvent peaks are marked with asterisks.

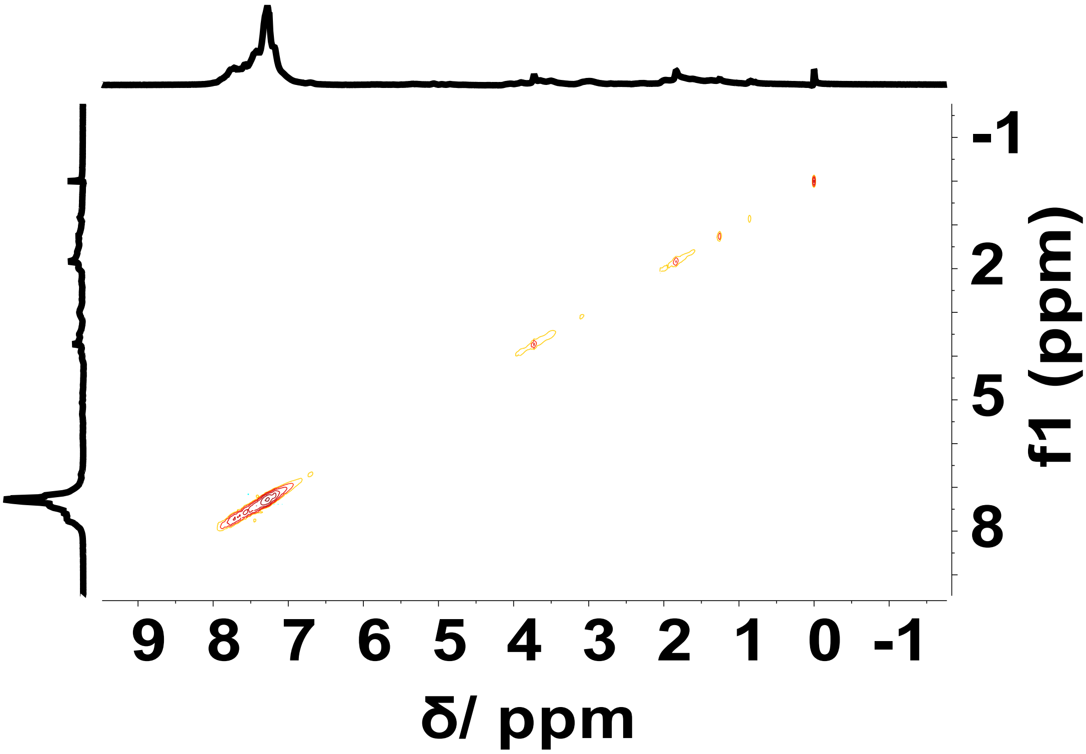

Figure S4. H-H cosy (400 MHz) NMR spectra of triphenylmethanol in $CDCl_3$.

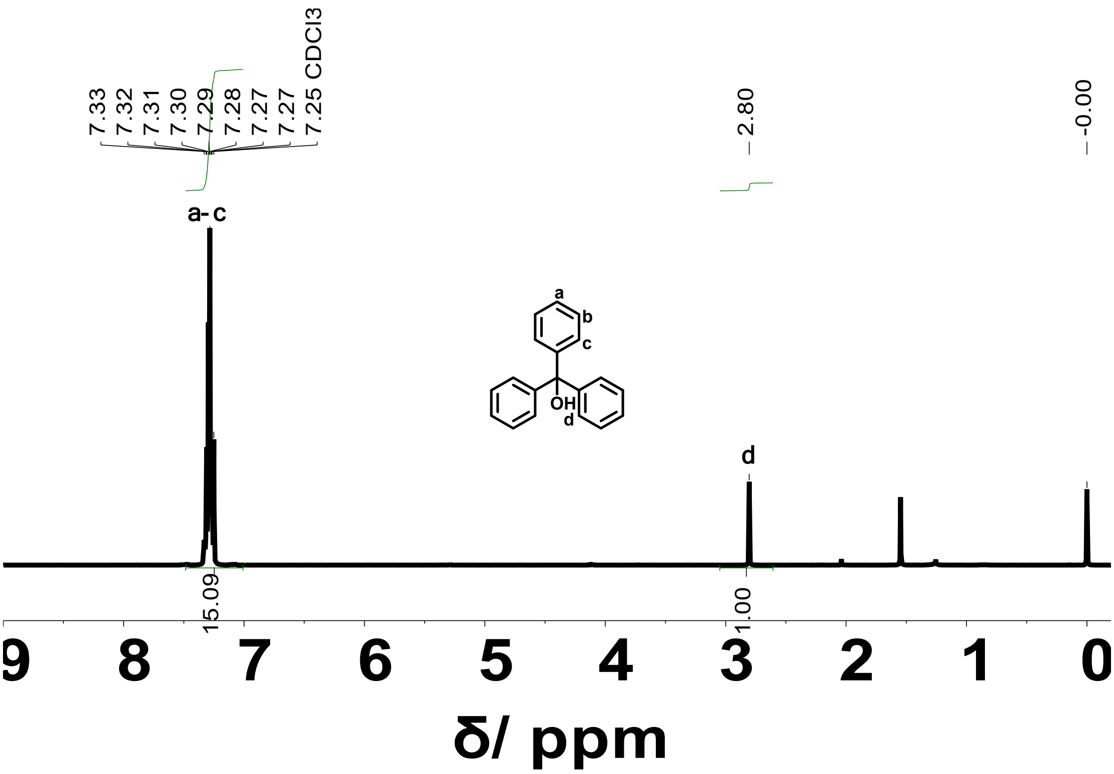

Figure S5. ^{1}H (400 MHz) NMR spectra of triphenylmethanol in $CDCl_3$.

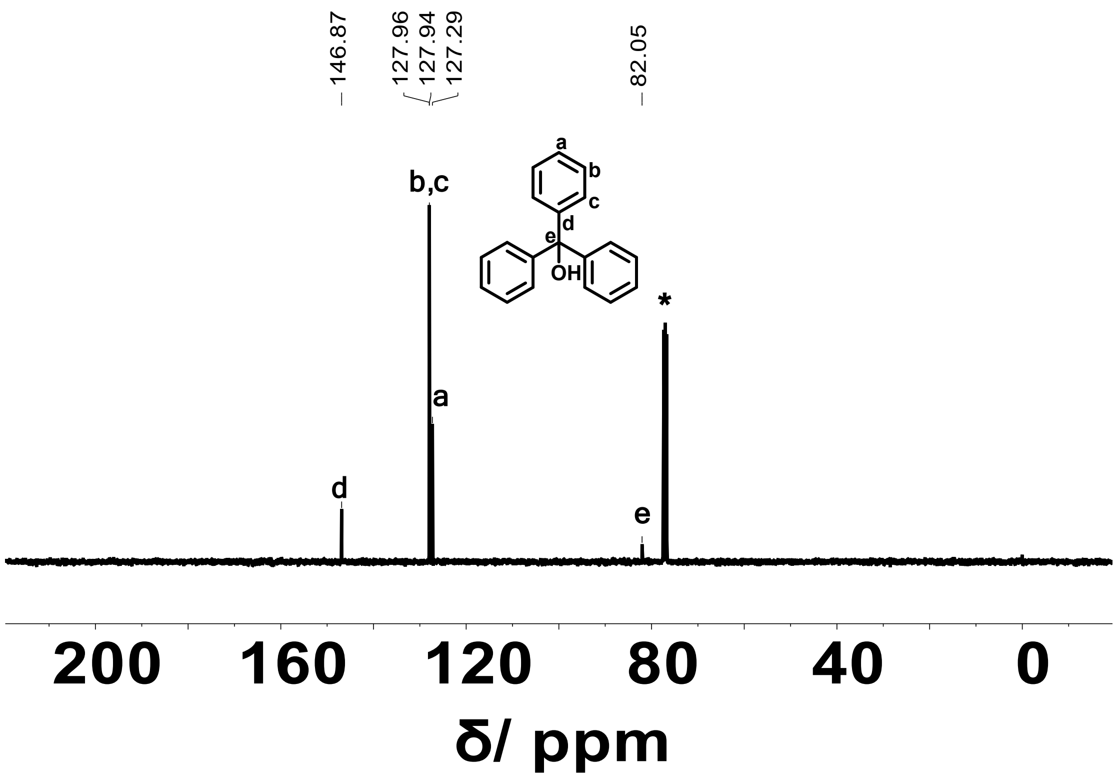

Figure S6. ^{13}C (100 MHz) NMR spectra of triphenylmethanol in $CDCl_3$. The solvent peaks are marked with asterisks.

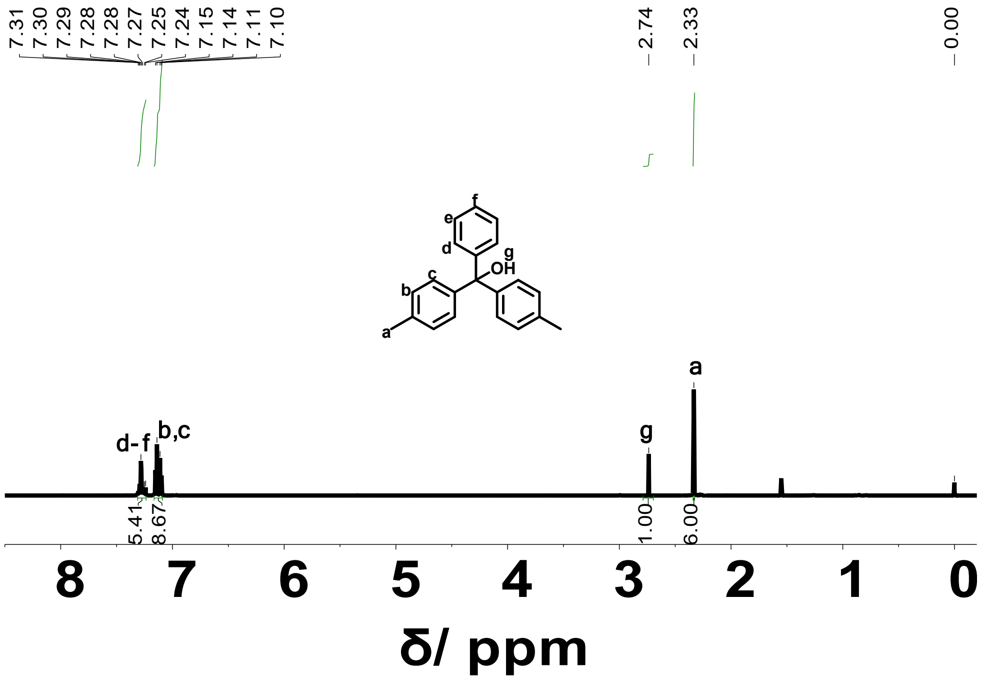

Figure S7. ^{1}H (400 MHz) NMR spectra of 4,4'-dimethyltriphenylmethanol in $CDCl_3$.

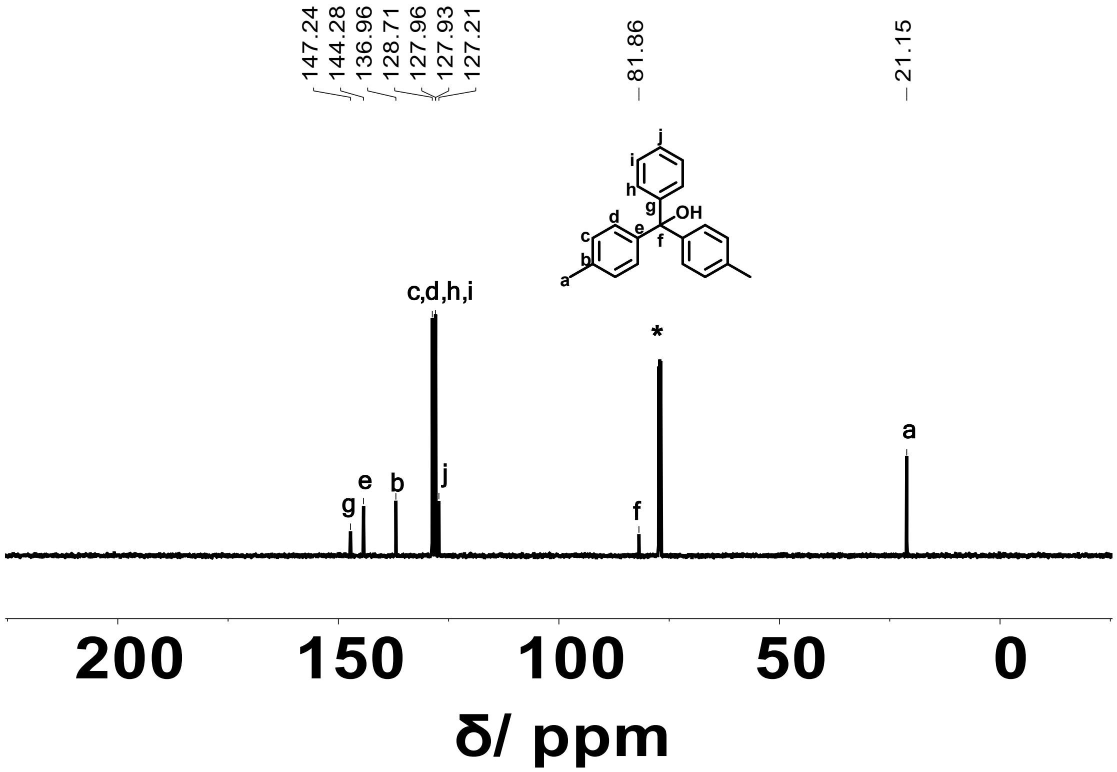

Figure S8. ^{13}C (100 MHz) NMR spectra of 4,4'-dimethyltriphenylmethanol in $CDCl_3$. The solvent peaks are marked with asterisks.

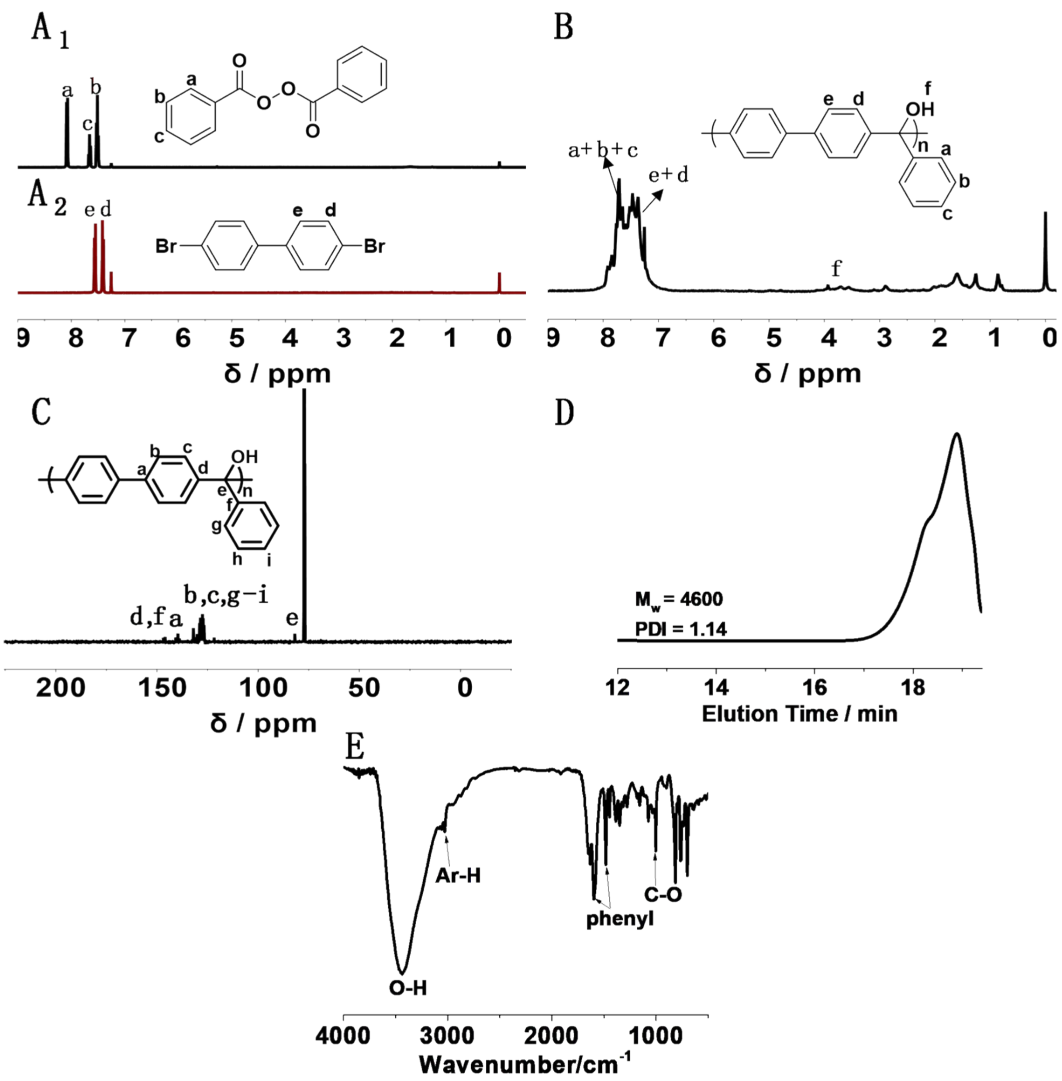

Figure S9. ^{1}H NMR spectra of benzoyl peroxide (A$_1$) and 4,4-dibromobiphenyl in CDCl$_3$ (A$_2$), ^{1}H NMR spectra (B), ^{13}C NMR(C), GPC curve (D) and FT-IR spectrum (E) of *p*-PPTPM.

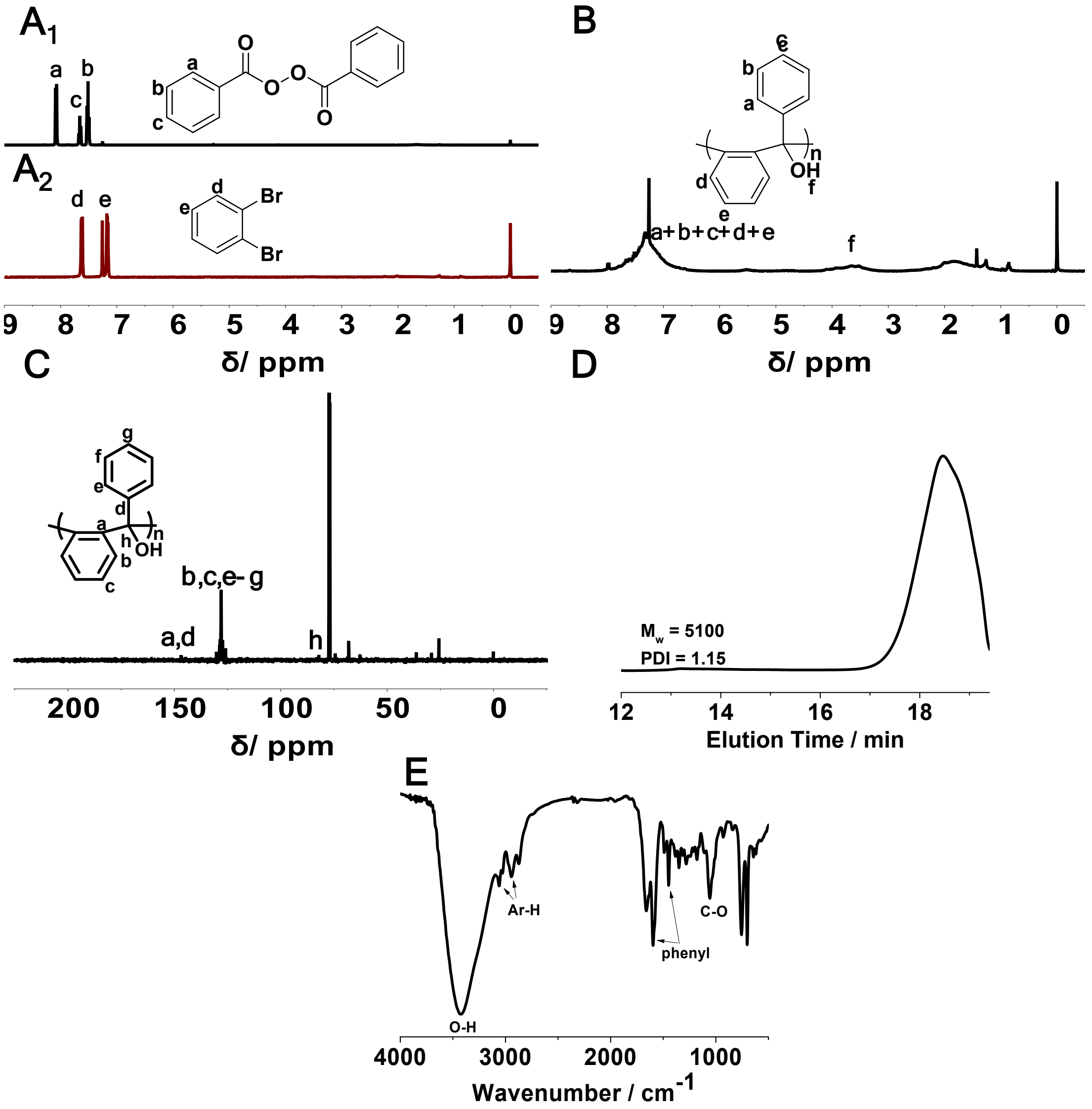

Figure S10. ^{1}H NMR spectra of benzoyl peroxide (A_1) and 1,2-dibromobenzene in $CDCl_3$ (A_2), ^{1}H NMR spectra (B), ^{13}C NMR(C), GPC curve (D) and FT-IR spectrum (E) of *o*-PTPM.

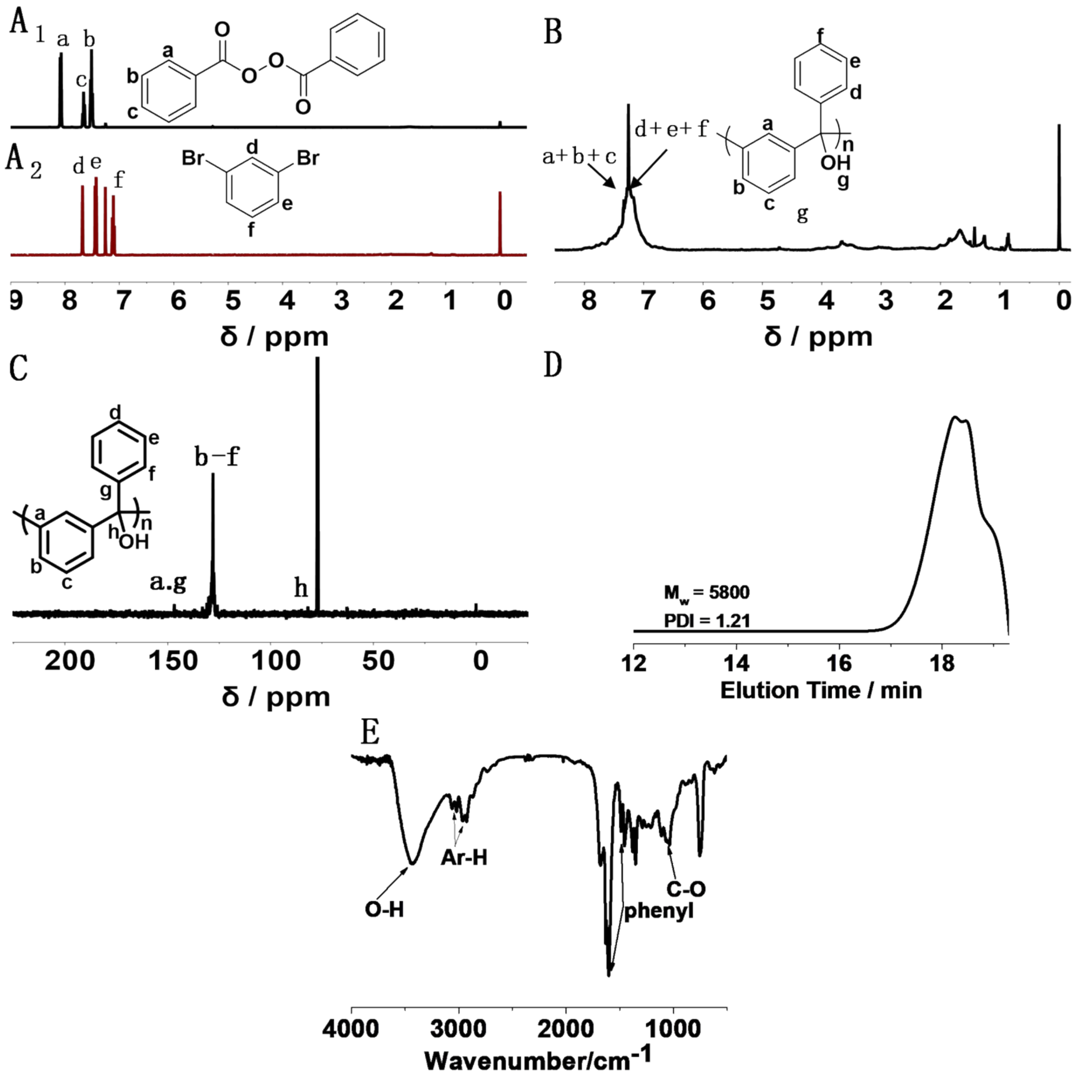

Figure S11. ^{1}H NMR spectra of benzoyl peroxide (A_1) and 1,3-dibromobenzene in $CDCl_3$ (A_2), ^{1}H NMR spectra (B), 13C NMR(C), GPC curve (D) and FT-IR spectrum (E) of *m*-PTPM.

Characterization of luminescent properties

Table S1. The photophysical data of polyphenylmethanols.

Entry	Structure	Abbreviation	λ_{abs} (nm)[a]	λ_{em} (nm)		FL[c]
				THF[b]	Solid	
1	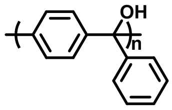	*p*-PTPM	265	-	468	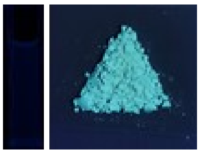
2	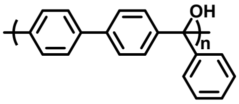	*p*-PPTPM	236	-	454	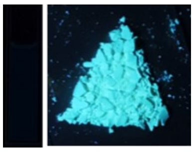
3	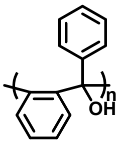	*o*-PTPM	237	438	-	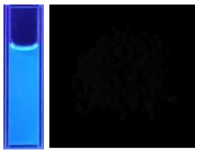
4	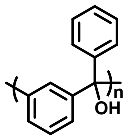	*m*-PTPM	236	391	-	

a. Maximum absorption wavelength;

b. Measured with 0.1 mg/mL solution in THF;

c. Photographs (under irradiation with UV lamp at 365 nm).

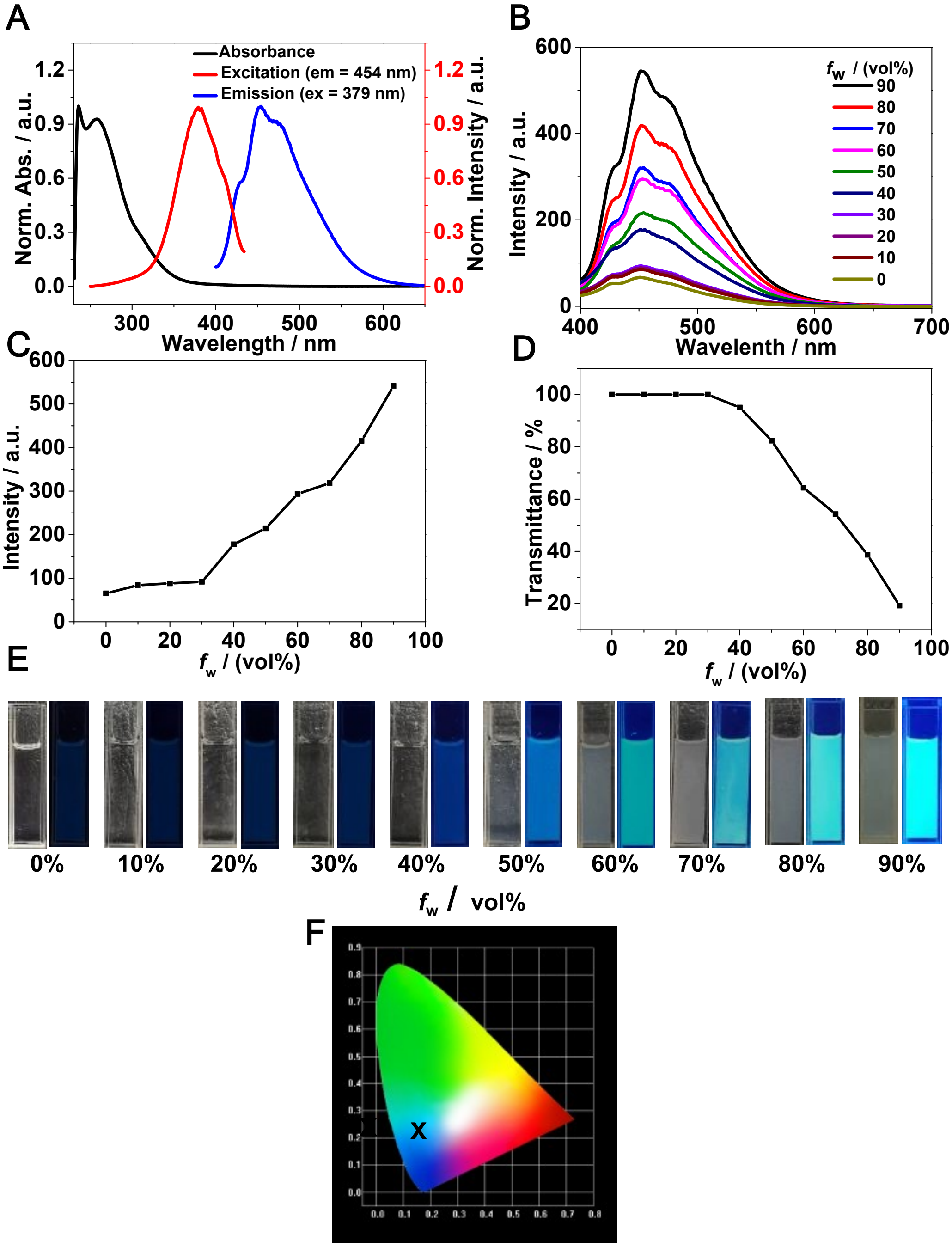

Figure S12. Luminescence properties of *p*-PPTPM. Normalized Excitation (red line) and emission (blue line) spectra of *p*-PPTPM in the solid state and normalized absorption spectra (black line) of *p*-PPTPM in THF (A). Emission spectra of *p*-PPTPM (0.1 mg/mL) in water/THF mixtures with different water volume fractions (f_w, vol %) (excited at 379 nm) (B). Plots of emission intensities of *p*-PPTPM (0.1 mg/mL) in water/THF mixtures with different water volume fractions (fw, vol %) (excited at 379 nm) (C). Transmittance of *p*-PPTPM (0.1 mg/mL) in water/THF mixtures with different water volume fractions (f_w, vol %) (D). Digital photos of *p*-PPTPM (0.1 mg/mL) in water/THF mixtures with different water volume fractions (f_w, vol %) (under sunlight and UV irradiation at 365 nm) (E). CIE coordinates of *p*-PPTPM (F).

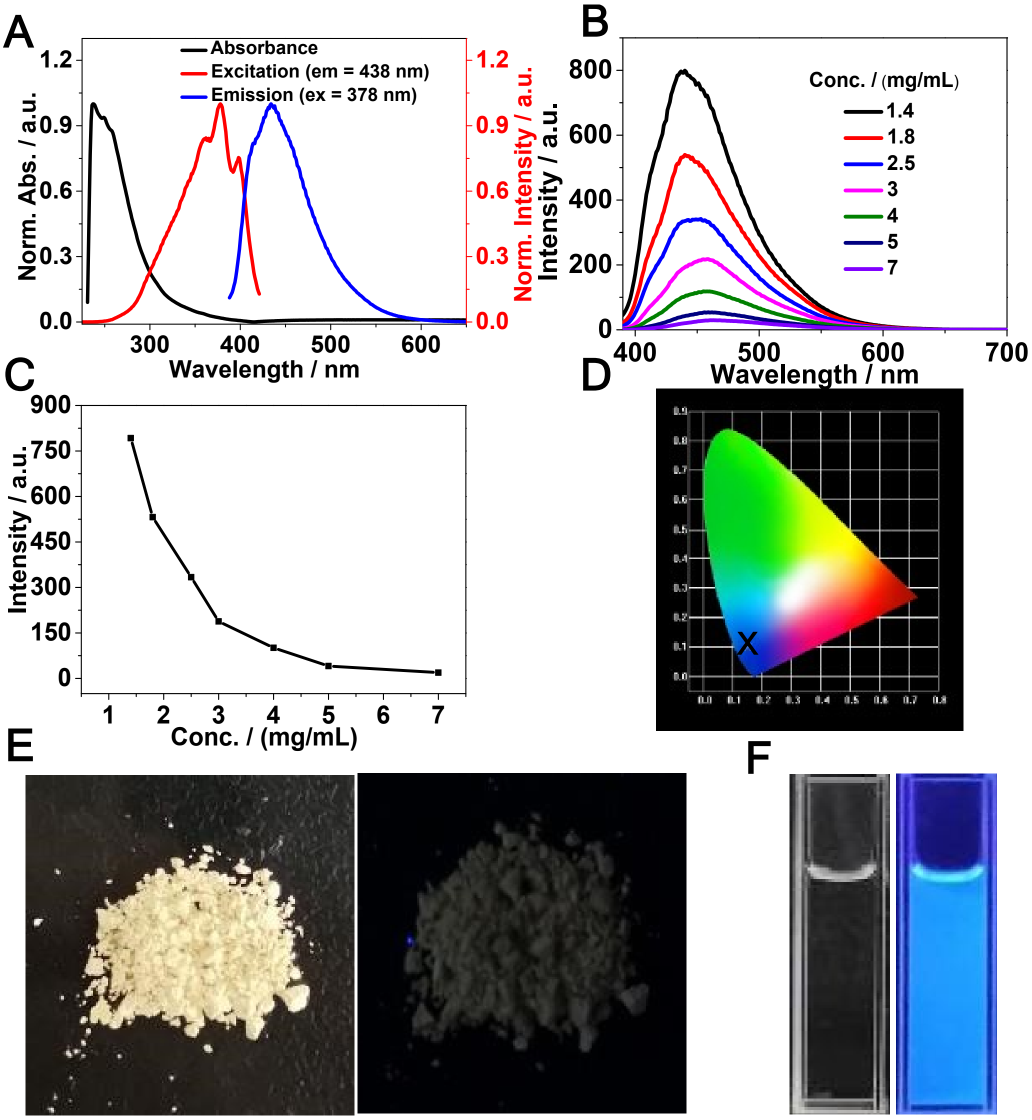

Figure S13. Luminescence properties of *o*-PTPM. Normalized Excitation (red line) and emission (blue line) spectra of *o*-PTPM in solution and normalized absorption spectra (black line) of *o*-PTPM in THF (A). The solution luminescence quenching curve (excited @ 378 nm). THF was chosen as the solvent used in the measurement. (B). Plots of emission intensities of *o*-PTPM with different concentration (excited at 378 nm) (C). CIE coordinates of *o*-PTPM (D). Digital photos of *o*-PTPM solid (under sunlight (left) and UV irradiation at 365 nm(right)) (E). Digital photos of *o*-PTPM solution in THF with 0.1mg/ mL (under sunlight (left) and UV irradiation at 365 nm (right)) (F).

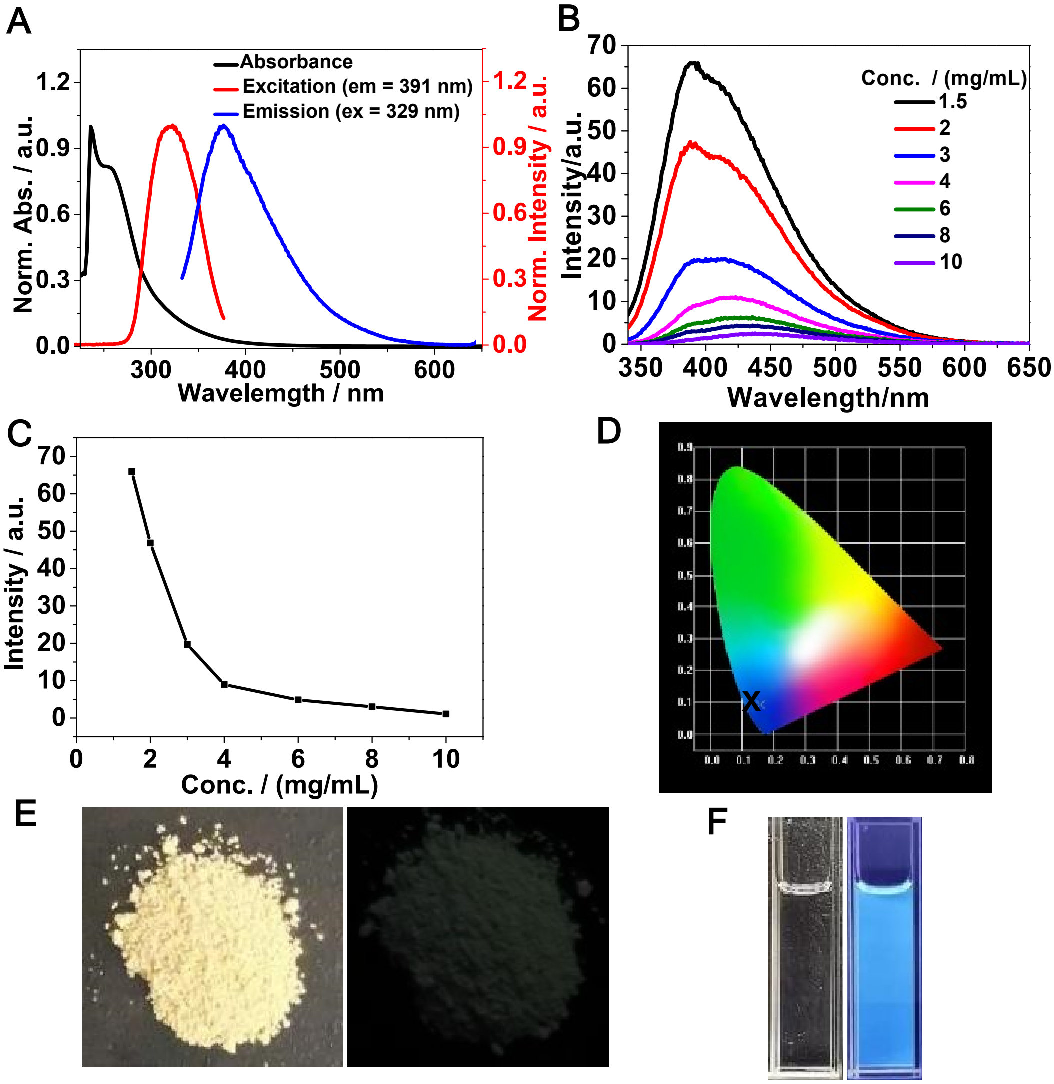

Figure S14. Luminescence properties of *m*-PTPM. Normalized Excitation (red line) and emission (blue line) spectra of *m*-PTPM in solution and normalized absorption spectra (black line) of *m*-PTPM in THF(A). The solution luminescence quenching curve (excited @ 378 nm). THF was chosen as the solvent used in the measurement. (B). Plots of emission intensities of *m*-PTPM with different concentration (excited at 378 nm) (C). CIE coordinates of *m*-PTPM (D). Digital photos of *m*-PTPM solid (under sunlight (left) and UV irradiation at 365 nm(right)) (E). Digital photos of *m*-PTPM solution in THF with 0.1mg/ mL (under sunlight (left) and UV irradiation at 365 nm(right)) (F).

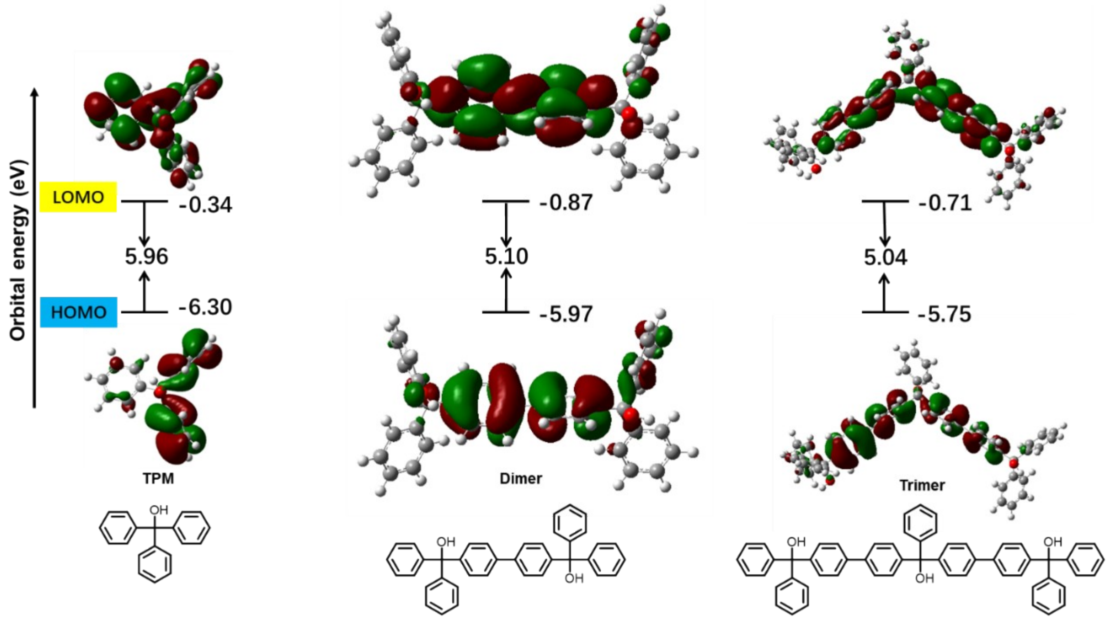

Figure S15. Electron cloud distributions and energy levels (eV) of TPM, dimer, trimer, in the geometry-optimized S1 state calculated by TD-DFT B3LYP/6-311G*, Gaussian 09 program.

Artificial light-harvesting system experiments

Energy-transfer efficiency

Energy-transfer efficiency, i.e., the fraction of the absorbed energy that is transferred to the acceptor, was experimentally measured as a ratio of the luminescence intensities of the donor in the absence and presence of the acceptor (I_D and I_{DA}).

$$\Phi_{ET} = 1 - \frac{I_{DA}}{I_D}$$

Antenna effect

The antenna effect under certain concentrations of donor and acceptor equals the ratio of the emission intensity at 620 nm of the acceptor upon excitation of the donor, $I_{A + D(\lambda ex = 386nm)}^{620nm} - I_{D(\lambda ex = 386nm)}^{620nm}$, that of the direct excitation of the acceptor, $I_{A + D(\lambda ex = 468nm)}^{620nm}$.

$$antenna\ effect = \frac{I_{A + D(\lambda ex = 386nm)}^{620nm} - I_{D(\lambda = 468nm)}^{620nm}}{I_{A + D(\lambda ex = 468nm)}^{620nm}}$$

Table S2. Results of energy-transfer efficiency and antenna effect of *p*-PTPM.

Entry	*p*-PTPM:NiR[a]	Φ_{ET}[b]	Antenna Effect
1	1000:1	30.3	7.8
2	1000:1.5	47.4	10.1
3	1000:2	56.0	10.1
4	1000:2.5	61.2	15.2
5	1000:3	66.6	18.5

a. mass ratios of *p*-PTPM/NiR, initial concentration: *p*-PTPM solution (10 mg/mL) in THF, NiR (1.0 mg/mL) in ethanol;

b. Φ_{ET} was calculated by a ratio of the luminescence intensities emitting at 468 nm of the *p*-PTPM as donor in the absence and presence of the acceptor.

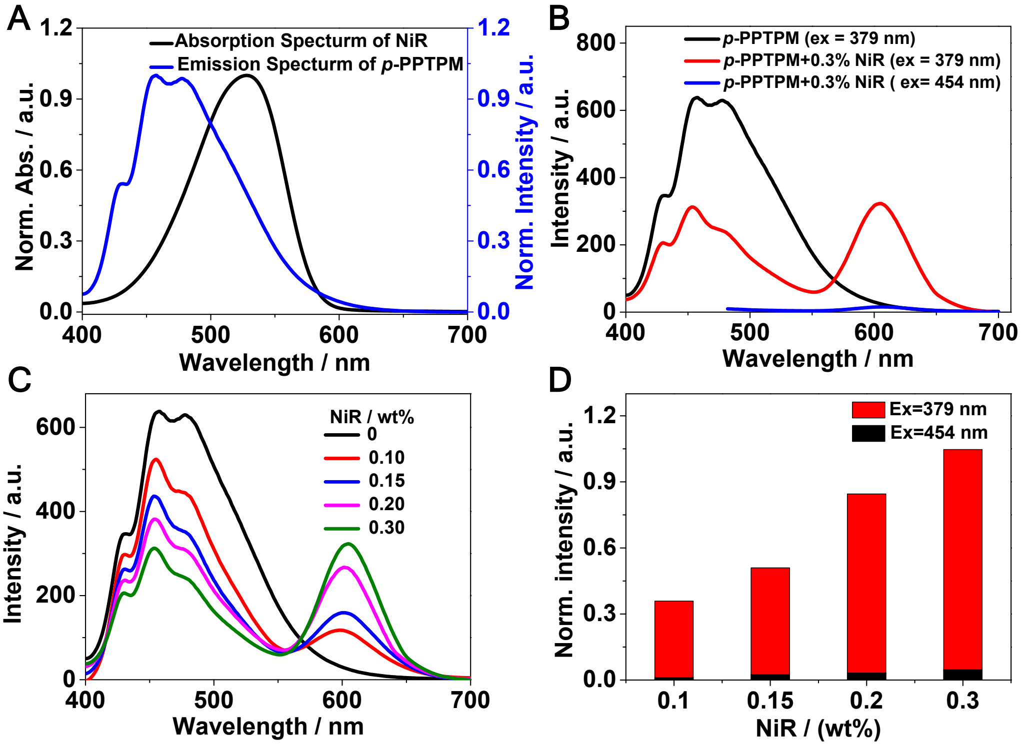

Figure S16. Artificial light-harvesting system application of *p*-PPTPM. Absorption spectra of NiR and emission spectra of *p*-PPTPM (ex = 386 nm) (A). Emission spectra of light-harvesting film using *p*-PPTPM as an energy donor, NiR as an energy acceptor (B). Emission spectra of light-harvesting films (C). Emission intensities (at 620 nm) of light-harvesting films (D).

Table S3. Results of energy-transfer efficiency and antenna effect of *p*-PTPM.

Entry	*p*-PPTPM:NiR[a]	Φ_{ET}[b]	Antenna Effect
1	1000:1	17.2	17.6
2	1000:1.5	30.9	15.3
3	1000:2	39.5	17.8
4	1000:3	50.5	18.1

a. mass ratios of *p*-PPTPM/NiR, initial concentration: PTPE solution (10 mg/mL) in THF, NiR (1.0 mg/mL) in ethanol;

b. Φ_{ET} was calculated by a ratio of the luminescence intensities emitting at 454 nm of the *p*-PPTPM as donor in the absence and presence of the acceptor.

Coordinate of optimized structures

Structure 1. TPM

$E(B3LYP)_{S1}$ = -808.68114955

C	-0.74184	1.23145	0.
C	0.65332	1.23145	0.
C	1.35086	2.4392	0.
C	0.6532	3.64771	-0.0012
C	-0.74162	3.64764	-0.00168
C	-1.43922	2.43943	-0.00068
H	-1.2916	0.27914	0.00045
H	1.20283	0.27894	0.00132
H	1.2034	4.59986	-0.00126
H	-1.29174	4.59992	-0.00263
H	-2.53883	2.43961	-0.00086
C	2.89086	2.43932	0.00089
C	3.40419	0.99885	0.18295
C	3.68318	0.21133	-0.93439
C	3.59033	0.4815	1.46484
C	4.14755	-1.09346	-0.76978
H	3.53559	0.61923	-1.94487
C	4.05579	-0.82333	1.62968
H	3.37067	1.10212	2.34559
C	4.33427	-1.61088	0.51265
H	4.36688	-1.71447	-1.65043
H	4.20285	-1.23083	2.64051
H	4.70048	-2.63967	0.64219
C	3.40346	3.31702	1.15781
C	4.44858	4.21559	0.94153
C	2.82287	3.21377	2.42185
C	4.91339	5.0102	1.98928
H	4.90661	4.2962	-0.05494
C	3.28704	4.00925	3.46978
H	1.99902	2.50574	2.59245
C	4.33222	4.90729	3.25374
H	5.73757	5.71803	1.81903
H	2.8288	3.92792	4.46621
H	4.69883	5.53395	4.07969
O	3.3682	2.96199	-1.24163
H	2.69359	2.85226	-1.91577

Structure 2. Dimer of TPM

E(B3LYP)$_{S1}$ = -1386.16393683

C	-3.96142	0.41543	0.
C	-2.56626	0.41543	0.
C	-1.86873	1.62318	0.
C	-2.56638	2.83169	-0.0012
C	-3.96121	2.83161	-0.00168
C	-4.65881	1.62341	-0.00068
H	-4.51118	-0.53689	0.00045
H	-2.01676	-0.53708	0.00132
H	-2.01618	3.78383	-0.00126
H	-4.51133	3.78389	-0.00263
H	-5.75841	1.62359	-0.00086
C	-0.32873	1.62329	0.00089
C	0.18461	0.18283	0.18295
C	0.46359	-0.60469	-0.93439
C	0.37075	-0.33452	1.46484
C	0.92797	-1.90948	-0.76978
H	0.316	-0.1968	-1.94487
C	0.8362	-1.63935	1.62968
H	0.15109	0.28609	2.34559
C	1.11469	-2.42691	0.51265
H	1.14729	-2.53049	-1.65043
H	0.98326	-2.04685	2.64051
C	0.18388	2.501	1.15781
C	1.22899	3.39956	0.94153
C	-0.39672	2.39774	2.42185
C	1.6938	4.19417	1.98928
H	1.68702	3.48018	-0.05494
C	0.06746	3.19323	3.46978
H	-1.22056	1.68971	2.59245
C	1.11264	4.09126	3.25374
H	2.51799	4.902	1.81903
H	-0.39078	3.1119	4.46621
H	1.47925	4.71793	4.07969
O	0.14862	2.14596	-1.24163
H	-0.52599	2.03623	-1.91577
C	1.62753	-3.86763	0.69406
C	1.79848	-4.52926	-0.68602
C	3.00143	-4.39487	-1.37978
C	0.75076	-5.26295	-1.24238
C	3.15631	-4.99351	-2.62993
H	3.82697	-3.81574	-0.94123
C	0.90588	-5.86266	-2.49246

H	-0.19736	-5.36912	-0.69564
C	2.10835	-5.72795	-3.18633
H	4.10424	-4.8871	-3.1771
H	0.07977	-6.44143	-2.9307
H	2.23072	-6.19991	-4.17202
C	0.61284	-4.67263	1.52712
C	1.00034	-5.23781	2.74239
C	-0.69358	-4.83663	1.0668
C	0.08173	-5.96739	3.49678
H	2.03058	-5.10899	3.10466
C	-1.61286	-5.56557	1.82177
H	-0.99921	-4.39109	0.10908
C	-1.22541	-6.13105	3.03653
H	0.38725	-6.41344	4.45438
H	-2.64297	-5.69437	1.45877
H	-1.94954	-6.70629	3.63154
O	2.88721	-3.84357	1.37047
H	3.28559	-4.71637	1.33708

Structure 3. Trimer of TPM

E(B3LYP)$_{S1}$ = -1961.64646668

C	-4.67359	0.86053	0.
C	-3.27843	0.86053	0.
C	-2.58089	2.06829	0.
C	-3.27855	3.27679	-0.0012
C	-4.67337	3.27672	-0.00168
C	-5.37097	2.06851	-0.00068
H	-5.22335	-0.09178	0.00045
H	-2.72892	-0.09198	0.00132
H	-2.72835	4.22894	-0.00126
H	-5.22349	4.229	-0.00263
H	-6.47058	2.06869	-0.00086
C	-1.04089	2.0684	0.00089
C	-0.52829	2.9461	1.15781
C	-0.09663	4.24883	0.90672
C	-0.49565	2.43877	2.4567
C	0.36819	5.04374	1.95423
H	-0.12177	4.64824	-0.11753
C	-0.03164	3.23413	3.50479
H	-0.83599	1.4121	2.6548
C	0.40038	4.53639	3.25376
H	0.70903	6.07036	1.7563
H	-0.0064	2.834	4.52887
H	0.76686	5.16336	4.07953
C	-0.52756	0.62793	0.18295
C	0.32664	0.0666	-0.76664
C	-0.91647	-0.11553	1.2972
C	0.79123	-1.23815	-0.60228
H	0.63244	0.65272	-1.64538
C	-0.45103	-1.42034	1.46227
H	-1.58956	0.32679	2.04582
C	0.40258	-1.98177	0.5127
H	1.46402	-1.68088	-1.35104
H	-0.75751	-2.00615	2.34112
O	-0.56355	2.59107	-1.24163
H	-1.13517	2.29592	-1.95419
C	0.91582	-3.42238	0.69393
C	-0.09862	-4.22775	1.52692
C	0.06253	-4.33548	2.90855
C	-1.17857	-4.84941	0.9002
C	-0.85575	-5.06528	3.66312
H	0.91447	-3.8459	3.40225
C	-2.09777	-5.57865	1.65498

H	-1.30583	-4.76446	-0.18871
C	-1.93647	-5.68679	3.03622
H	-0.72846	-5.15076	4.75206
H	-2.9494	-6.06835	1.16062
H	-2.6604	-6.26211	3.63139
C	1.0869	-4.0838	-0.68624
C	2.33925	-4.55189	-1.08498
C	-0.01013	-4.21503	-1.53762
C	2.49458	-5.15044	-2.33511
H	3.20409	-4.44759	-0.41385
C	0.14487	-4.81462	-2.78776
H	-0.99728	-3.84632	-1.22343
C	1.39698	-5.28219	-3.18667
H	3.48179	-5.51884	-2.64973
H	-0.72036	-4.91832	-3.45866
O	2.17552	-3.39806	1.37029
H	2.48182	-4.29715	1.50967
C	1.56882	-5.94322	-4.56693
C	0.37654	-6.87891	-4.83999
C	0.34277	-8.15088	-4.26777
C	-0.66963	-6.45477	-5.65925
C	-0.73663	-8.9987	-4.51536
H	1.16807	-8.48525	-3.62255
C	-1.74991	-7.30236	-5.90622
H	-0.64326	-5.45222	-6.11018
C	-1.78351	-8.57421	-5.33456
H	-0.76302	-10.00153	-4.06488
H	-2.57482	-6.96752	-6.55188
H	-2.6345	-9.24284	-5.52958
C	1.62609	-4.85406	-5.65416
C	2.83786	-4.55277	-6.2765
C	0.46655	-4.16886	-6.01681
C	2.89012	-3.56602	-7.26078
H	3.75199	-5.09261	-5.98982
C	0.51846	-3.18246	-7.00207
H	-0.48863	-4.40632	-5.52653
C	1.73	-2.88086	-7.62397
H	3.84533	-3.32805	-7.75092
H	-0.39602	-2.64266	-7.28809
H	1.77143	-2.10292	-8.40011
O	2.7823	-6.69953	-4.58549
H	2.82298	-7.22039	-5.39087

Structure 4. Tetramer of TPM

$E(B3LYP)_{S1}$ = -2358.13065745

C	-5.08902	0.96439	0.
C	-3.69386	0.96439	0.
C	-2.99632	2.17214	0.
C	-3.69398	3.38065	-0.0012
C	-5.0888	3.38057	-0.00168
C	-5.7864	2.17237	-0.00068
H	-5.63878	0.01207	0.00045
H	-3.14435	0.01188	0.00132
H	-3.14378	4.33279	-0.00126
H	-5.63892	4.33285	-0.00263
H	-6.88601	2.17255	-0.00086
C	-1.45632	2.17225	0.00089
C	-0.94299	0.73179	0.18295
C	-0.66401	-0.05573	-0.93439
C	-0.75685	0.21444	1.46484
C	-0.19963	-1.36052	-0.76978
H	-0.81159	0.35217	-1.94487
C	-0.2914	-1.09039	1.62968
H	-0.97651	0.83505	2.34559
C	-0.01291	-1.87794	0.51265
H	0.01969	-1.98153	-1.65043
H	-0.14433	-1.49789	2.64051
H	0.3533	-2.90673	0.64219
C	-0.94372	3.04996	1.15781
C	0.1014	3.94852	0.94153
C	-1.52431	2.9467	2.42185
C	0.5662	4.74313	1.98928
H	0.55943	4.02914	-0.05494
C	-1.06014	3.74219	3.46978
H	-2.34816	2.23867	2.59245
C	-0.01496	4.64022	3.25374
H	1.39039	5.45097	1.81903
H	-1.51838	3.66086	4.46621
O	-0.97898	2.69492	-1.24163
H	-1.6536	2.58521	-1.91576
C	0.49845	5.51781	4.4104
C	1.85505	6.1353	4.0232
C	1.90117	7.38223	3.39909
C	3.03766	5.44808	4.29651
C	3.12963	7.94143	3.04781
H	0.9686	7.92342	3.18306
C	4.26663	6.00775	3.94608

H	3.00151	4.46537	4.78856
C	4.31279	7.25417	3.32169
H	3.16603	8.92399	2.55531
H	5.19893	5.46586	4.16207
C	0.66958	4.65366	5.67355
C	-0.06241	4.94772	6.82429
C	1.55626	3.57695	5.6672
C	0.09282	4.1656	7.96859
H	-0.76079	5.79712	6.82922
C	1.71092	2.79389	6.81146
H	2.13313	3.34494	4.76027
C	0.97949	3.08811	7.9621
H	-0.48364	4.3977	8.87585
H	2.40979	1.94477	6.80603
H	1.10167	2.47154	8.86444
O	-0.44344	6.56175	4.67105
H	-0.06237	7.19037	5.28849
C	5.66906	7.87194	2.93376
C	5.52554	8.62961	1.60074
C	5.08163	9.95225	1.59448
C	5.83942	7.99366	0.39966
C	4.95102	10.63849	0.38732
H	4.83351	10.4531	2.5415
C	5.70977	8.68028	-0.80787
H	6.18948	6.95127	0.40443
C	5.26552	10.00245	-0.81425
H	4.60053	11.68081	0.38226
H	5.95772	8.17873	-1.75468
H	5.16251	10.54375	-1.76592
C	6.12115	8.85	4.03404
C	7.35407	8.67171	4.66221
C	5.29813	9.91414	4.40254
C	7.76349	9.55702	5.65911
H	8.00235	7.83222	4.37201
C	5.70797	10.80038	5.39904
H	4.32644	10.0549	3.90742
C	6.94037	10.62193	6.02743
H	8.735	9.4162	6.15473
H	5.05902	11.63956	5.68909
O	6.64193	6.83384	2.78964
H	7.49026	7.21946	2.55892
C	7.39278	11.59933	7.12816
C	6.34166	12.71324	7.28927
C	6.36756	13.82405	6.44553

C	5.36367	12.61161	8.27859
C	5.41607	14.83328	6.59159
H	7.13919	13.90424	5.66616
C	4.41122	13.62059	8.42419
H	5.343	11.7361	8.94356
C	4.43734	14.73139	7.58099
H	5.43681	15.70916	5.92699
H	3.63998	13.53999	9.20405
H	3.68719	15.52723	7.69593
C	8.7455	12.22271	6.73684
C	9.86089	12.03875	7.55448
C	8.85567	12.97112	5.56497
C	11.08598	12.60368	7.20059
H	9.77353	11.44931	8.47869
C	10.0813	13.53546	5.21032
H	7.97671	13.11606	4.92033
C	11.19635	13.35199	6.02796
H	11.96504	12.45925	7.84533
H	10.16796	14.12516	4.28608
H	12.16241	13.79727	5.74911
O	7.53281	10.89372	8.36405
H	7.88531	11.48548	9.03275